Drug Design, Development and Therapy

Dovepress
Taylor & Francis Group

Open Access Full Text Article

ORIGINAL RESEARCH

Ginsenoside Rg1 Ameliorates Pulmonary Hypertension by Inhibiting cGAS/STING Mediated Cell Senescence

Rongzhen Ding[1–3], Haiping Xie[4], Yu Zhang[2,3], Li Qin[3,5], Guoran Peng[2,3], Jian Yi[2,3], Junlan Tan[6], Xianya Cao[2,3], Runxiu Zheng[2,3], Aiguo Dai[2]

[1]Department of Health Management, The First Hospital of Hunan University of Chinese Medicine, Changsha, Hunan, 410021, People's Republic of China; [2]Department of Respiratory Diseases, Medical School, Hunan University of Chinese Medicine, Changsha, Hunan, 410208, People's Republic of China; [3]Hunan Provincial Key Laboratory of Vascular Biology and Translational Medicine, Changsha, Hunan, 410208, People's Republic of China; [4]Department of Urology, The First Hospital of Hunan University of Chinese Medicine, Changsha, Hunan, 410021, People's Republic of China; [5]Laboratory of Stem Cell Regulation with Chinese Medicine and Its Application, School of Pharmacy, Hunan University of Chinese Medicine, Changsha, Hunan, 410208, People's Republic of China; [6]Department of Gerontology, The First Hospital of Hunan University of Chinese Medicine, Changsha, Hunan, 410021, People's Republic of China

Correspondence: Aiguo Dai, Department of Respiratory Diseases, Medical School, Hunan University of Chinese Medicine, Changsha, Hunan, 410208, People's Republic of China, Tel +86 0731-88459072, Email daiaiguo@hnucm.edu.cn

Background: Pulmonary hypertension (PH) is a fatal pulmonary vascular disease that currently lacks effective treatment methods. Ginsenoside Rg1 has positive effects on improving PH, but its specific mechanism remains unclear.

Purpose: This study was designed to investigate the molecular mechanisms of ginsenoside Rg1 in improving PH.

Methods: The therapeutic efficacy of ginsenoside Rg1 in PH rat model was assessed using cardiopulmonary hemodynamic measurements and histopathological staining. Network pharmacology analysis was used to predict potential targets, and the expression of cyclic GMP–AMP synthase (cGAS)/stimulator of interferon genes (STING) pathway proteins was evaluated by immunofluorescence staining. Senescence marker gene transcription and protein levels were assessed by RT-PCR and immunohistochemistry, respectively. Finally, ELISA was employed to quantify senescence-associated secreted proteins (SASP).

Results: Our results demonstrate that ginsenoside Rg1 significantly reduces right ventricular systolic pressure (RVSP). Ultrasound findings indicate that ginsenoside Rg1 increases the pulmonary artery acceleration time to pulmonary ejection time ratio (PAT/PET) and tricuspid annular plane systolic excursion (TAPSE), while reducing the right ventricular anterior wall thickness (RVAWT). Histological examination (HE) suggests that ginsenoside Rg1 significantly diminishes pulmonary vascular remodeling. Furthermore, ginsenoside Rg1 markedly decreases the mRNA and protein expression of the aging markers p21 and p16, as well as significantly reduces the NF-kB, IL-6, and IL-8.

Conclusion: This study presents compelling evidence that ginsenoside Rg1 may enhance pulmonary vascular remodeling in PH by inhibiting cell senescence via the cGAS/STING signaling pathway.

Keywords: ginsenoside Rg1, pulmonary hypertension, cGAS/STING signaling pathway, cell senescence, pulmonary vascular remodeling

Introduction

Pulmonary Hypertension (PH) is a severe cardiovascular disorder that poses a significant threat to human health, affecting approximately 1% of the global population and up to 10% of individuals aged 65 years and older.[1] Persistent and irreversible pulmonary vascular remodeling (PVR) is the hallmark pathological alteration of PH.[2] The pathological changes of PH primarily manifest as thickening of distal pulmonary arteriolar walls and luminal stenosis, leading to increased pulmonary vascular resistance and pulmonary arterial pressure, subsequently triggering right ventricular hypertrophy, which may ultimately result in fatal right heart failure.[3,4] Despite recent advances in understanding the

Received: 12 March 2025
Accepted: 22 July 2025
Published: 29 July 2025

pathogenesis of PH, the complex nature of its pathological mechanisms has limited the efficacy of current therapeutic strategies, resulting in high patient mortality rates.[5,6] Therefore, elucidating the underlying pathogenic mechanisms of PH and identifying new treatments is crucial for better prognosis and treatment.

Cellular senescence is a permanent blockage of cell cycle progression, resulting in the loss of the cell's ability to divide and proliferate, and can be triggered by factors such as telomere shortening, oxidative stress, and DNA damage.[7] Cellular senescence manifests in two primary forms: replicative senescence and stress-induced premature senescence.[8] Replicative senescence occurs due to progressive telomere attrition during cellular proliferation, triggering a DNA damage response cascade.[9] In contrast, stress-induced premature senescence is initiated by exogenous stressors, including oxidative stress and radiation, leading to premature cellular senescence.[10,11] While both forms exhibit similar morphological and molecular characteristics, stress-induced premature senescence typically proceeds independently of telomere erosion.[12] Cellular senescence plays a pivotal role in PH pathogenesis. Pulmonary artery smooth muscle cells (PASMCs), critical cellular constituents of the pulmonary vascular media, undergo cellular senescence upon exposure to environmental stimuli, including smoke, particulate matter, hypoxic conditions, and inflammatory factors.[13,14] The senescence-associated secretory phenotype (SASP) encompasses a diverse array of secreted factors, including cytokines, chemokines, extracellular matrix proteases, growth factors, and other signaling molecules produced by senescent cells.[15] Senescent PASMCs contribute to PH pathogenesis by modulating cell cycle dysregulation and through the SASP, which affects proliferation, apoptosis, and migratory behavior in both senescent cells and their non-senescent neighbors.[16]

The cyclic GMP-AMP synthase (cGAS)/stimulator of interferon genes (STING) pathway represents a crucial component of innate immunity, specifically mediating cytoplasmic nucleic acid recognition.[17] cGAS recognizes aberrantly released mitochondrial DNA (mtDNA) and subsequently activates STING, triggering multiple downstream signaling cascades that modulate diverse cellular functions.[18] Recent studies have revealed that the cGAS/STING pathway exerts broad effects on cardiovascular diseases, aging, and cancer.[19–21] Mitochondrial damage in PASMCs triggers the release of superoxide and mitochondrial DNA (mtDNA), subsequently activating the cGAS/STING/NFκB signaling cascade to promote PH progression.[22] Furthermore, targeting the mtDNA/cGAS/STING signaling pathway can inhibit PASMCs proliferation and phenotypic transformation, thereby exerting therapeutic effects against PH.[23] However, the molecular mechanisms by which the cGAS/STING pathway regulates PASMCs senescence in PH remain incompletely understood.

Ginseng (Panax ginseng C. A. Meyer), a perennial herb of the Araliaceae family (genus Panax), has a long history of use in traditional Chinese medicine.[24,25] Modern research identifies ginsenosides as its primary bioactive compounds, with ginsenoside Rg1 being the most studied due to its diverse pharmacological effects, including anti-aging, anti-inflammatory, and antitumor activities.[26–28] Ginsenoside Rg1 activates the FAK/AKT–FOXO3A pathway to significantly mitigate sepsis-induced myocardial injury in mice, reducing cardiomyocyte apoptosis, inflammation, and iron accumulation.[29] Ginsenoside Rg1 ameliorates cardiac arrest and cardiopulmonary resuscitation-induced cognitive impairment in rats by restoring synaptic structure and function.[30] It attenuates reactive oxygen species production and cellular apoptosis while enhancing antioxidant enzyme activity, thereby decelerating the senescence.[31] In addition, ginsenoside Rg1 administration enhances autophagic activity and attenuates paraquat-induced pulmonary fibrosis while mitigating both cellular senescence and the SASP through upregulation of ATG12 expression.[31] Ginsenoside Rg1 treatment was reported to ameliorate PH by regulating CCN1 expression, thereby reversing hypoxia-induced endothelial-to-mesenchymal transition and inflammatory responses.[32] In the present study, a hypoxia / Sugen PH model was established to evaluate the therapeutic effects of RG-1 and investigate the mechanism of cGAS/STING pathway-mediated cellular senescence in PVR, providing new insights for the treatment of PH.

Materials and Methods

Chemicals and Reagents

Ginsenoside Rg1 (RS02541020) was purchased from Shanghai Standard Technology Co., Ltd. Sidenafil and Sugen were available from Selleck (S1431) and MedChemExpress (HY-10374), respectively. Antibodies against cyclic GMP–AMP

synthase (cGas, PA5-121188), STING (PA5-23381), pSTING (PA5-105674), TANK-binding kinase 1 (TBK1, MA1-20344), pTBK1 (PA5-105919), p16 (PA5-20379), and p21 (14–6715-81) were obtained from ThermoFisher Scientific. Antibody against α-smooth muscle actin (α-SMA, 19245) and proliferating cell nuclear antigen (PCNA, 13110) was purchased from CST.

PH Rodent Model

Eight-week-old male rats were purchased from Hunan SJA Laboratory Animal Co., Ltd. (Changsha, Hunan, China, License No. CXK (Xiang) 2019–004). The rats were housed at the Animal Center of Hunan University of Chinese Medicine. After a one-week acclimatization period, the experimental animals were subjected to combined hypoxic treatment and sugen administration. By dynamically introducing N_2, the oxygen concentration in the chamber was maintained at 10%±0.5%. The experimental rats were treated with hypoxia for 8 hours per day over a period of three weeks. A single subcutaneous injection of sugen (20 mg/kg/week) was administered to rats before a three-week hypoxic exposure. Sample size was determined by power analysis (Cohen's d ≈1.83), yielding n = 6 per group for 80% power at α = 0.05. To account for potential attrition, n = 8 per group was used. The rats were divided into 6 groups: normoxia control group (CTR), hypoxia combined with sugen model group (SuHx), SuHx+ Ginsenoside Rg1 low-dose group (Rg1 L, 10 mg/kg/d), SuHx+ Ginsenoside Rg1 medium-dose group (Rg1 M, 15 mg/kg/d), SuHx+ Ginsenoside Rg1 high-dose group (Rg1 H, 20 mg/kg/d), SuHx+ Positive control drug Sildenafil (SIL, 25mg/kg/d). Ginsenoside Rg1 or Sildenafil was dissolved in 5% sodium carboxymethyl cellulose and gavaged to rats for 3 weeks. Cardiopulmonary hemodynamic testing was conducted, and lung tissue and serum were collected after three weeks. All animal procedures were approved by the Ethics Committee of The First Hospital of Hunan University of Chinese Medicine and carried out in strict accordance with the Guide for the Care and Use of Laboratory Animals.[33]

Hemodynamic Analysis

The external jugular vein right heart catheterization method was used to detect RVSP in rats by MP160 BIOPAC multi-channel physiological monitoring system. Rats were anesthetized using isoflurane inhalation. The pulmonary artery acceleration time (PAAT), pulmonary ejection time (PET), tricuspid annular plane systolic excursion (TAPSE), and right ventricular anterior wall thickness (RVAWT) were measured using a small-animal ultrasound Doppler.

Hematoxylin-Eosin (H&E) Staining

Tissue sections were deparaffinized and rehydrated through a graded series of ethanol to distilled water. Hematoxylin stain was applied for 10 minutes, followed by rinsing in tap water. Differentiation was performed using 1% hydrochloric acid in alcohol for 30 seconds, and sections were immersed in water for 15 minutes. Eosin staining followed, and the sections were then dehydrated, cleared, and sealed with neutral resin.

Routine Blood Tests and Biochemical Detection

Blood samples were collected from the abdominal aorta and immediately subjected to centrifugation at 1,000 ×g for 20 min at 4°C to separate serum. Routine hematological parameters were analyzed using a Sysmex XE-2100 automated hematology analyzer (Sysmex Corporation, Kobe, Japan). Serum levels of creatinine (Cr), blood urea nitrogen (BUN), aspartate aminotransferase (AST), and alanine aminotransferase (ALT) were measured with a Hitachi 7600 Autoanalyzer (Hitachi Ltd., Tokyo, Japan) according to the manufacturer's protocols.

Target Identification and Network Pharmacology Analysis

All analyses involving publicly available human datasets were reviewed and approved by the Ethics Committee of The First Hospital of Hunan University of Chinese Medicine. Disease-associated targets related to "Pulmonary Hypertension" were retrieved from publicly accessible databases, including GeneCards (https://www.genecards.org) and OMIM (https://omim.org). The acquired targets were merged, followed by deduplication and gene symbol normalization using the UniProt database (https://www.uniprot.org) to standardize nomenclature. The 2D/3D chemical structure of Ginsenoside Rg1 was obtained from PubChem (https://pubchem.ncbi.nlm.nih.gov), and its

potential human-specific (Homo sapiens) targets were predicted using SwissTargetPrediction (http://www.swisstargetprediction.ch) and the SEA database (https://sea.bkslab.org). Common targets between PH-associated genes and Rg1-predicted targets were identified via a Venn diagram generated with Venny 2.1 (https://bioinfogp.cnb.csic.es/tools/venny). These overlapping genes were analyzed through the STRING database (https://string-db.org) under Homo sapiens-specific parameters (confidence score threshold >0.4) to construct a protein-protein interaction (PPI) network, which was subsequently visualized and analyzed using Cytoscape 3.9.1. Functional enrichment analysis of the overlapping targets—encompassing Gene Ontology (GO) terms and KEGG pathways—was conducted via the DAVID database (https://david.ncifcrf.gov), with a significance threshold of $p<0.05$.

Molecular Docking

Protein structures were retrieved from the Protein Data Bank (RCSB PDB, http://www.rcsb.org/pdb/) in PDB format. The structural files were pre-processed using PyMOL software to remove water molecules and ions. Hydrogen atoms were added, polar hydrogens were optimized, and partial charges were assigned using AutoDockTools. The final prepared receptor structure was converted into PDBQT format. Small molecule ligands were obtained in SDF format from the PubChem database (https://pubchem.ncbi.nlm.nih.gov/), geometry-optimized in Chem3D Pro for minimal energy conformation, and converted to MOL files prior to PDBQT conversion using OpenBabel utilities. Molecular docking was performed with Vina, utilizing the binding pocket coordinates specified in the PDB files as the target site.

Wheat Germ Agglutinin (WGA) Staining

After euthanizing the rats, cardiac tissues were collected and fixed with 4% paraformaldehyde. Samples were dehydrated in a graded ethanol series from 70% to 100%. Next, WGA-AF488 staining solution (W11261, ThermoFisher) was used dropwise to each tissue section incubating overnight at 4°C. Subsequently, DAPI staining was performed for 30 minutes. Finally, the slides were mounted and observed under a fluorescence microscope.

Fulton Index

Right ventricular hypertrophy was quantified by Fulton's index, derived by comparing the mass of the right ventricle with the combined mass of the left ventricle and septum, expressed as RV/(LV+S).

Immunofluorescence

Lung tissue sections, approximately 4 μm thick, were deparaffinized and hydrated sequentially. Antigen retrieval was then performed, followed by the application of an autofluorescence quencher for 5 minutes and washing with running water for 10 minutes. Subsequently, BSA was applied for 30 minutes. Sections were exposed to the primary antibodies Anti-PCNA, Anti-α-SMA, Anti-cGAS, and Anti-STING, and were incubated overnight at 4°C. Following washing, the sections were incubated with the appropriate secondary antibodies for 50 minutes. After rinsing, the nuclei were counterstained with DAPI, and finally, the sections were sealed with an antifluorescence quenching agent and examined under a microscope.

Immunohistochemistry Staining

Rat lung tissue sections underwent antigen retrieval, followed by the application of endogenous peroxidase inhibitors and blocking at 22–23°C. The sections were then incubated with primary and secondary antibodies targeting p16 and p21. Subsequently, DAB staining was carried out, followed by nuclear counterstaining.

Quantitative Real-Time PCR (RT-qPCR)

Total pulmonary vascular RNA was purified using trizol (15596018CN, ThermoFisher) following the manufacturer's instructions. Reverse transcription and quantitative real-time PCR (qRT-PCR) were performed according to previously established methods. All primer sequences used in this study are listed in Table S1.

ELISA

The serum was separated by centrifugation after whole blood was collected from the abdominal aorta of rats and left to stand for 2 hours at room temperature. The diluted serum was added to ELISA plate wells at 100 μL per well and incubated at 37°C for 90 minutes. Biotinylated antibody was included at 100 μL and incubated at 37°C for 1 hour. Following washing, 100 μL of HRP enzyme marker was added and incubated at 37°C for 30 minutes. The substrate solution was added 90 μL and incubated at 37°C for 15 min avoiding light. After the reaction was terminated, the OD value was measured with an enzyme labeler at 450 nm. IL-6 (E-EL-R0015) and NF-kB (E-EL-R0673) were obtained from Elabscience Biotechnology, and IL-8 (ab273236) was purchased from Abcam.

Western Blot

Protein extraction and Western blotting were performed as previously described.[34] Lung tissues were homogenized in RIPA buffer with protease and phosphatase inhibitors on ice, then centrifuged. Supernatants were quantified by BCA assay, and 20 μg of protein was separated by SDS–PAGE and transferred to PVDF membranes. Membranes were blocked, incubated with primary antibodies at 4 °C, washed, and then incubated with HRP-conjugated secondary antibodies. Bands were detected using ECL and imaged. Signal intensities were quantified in ImageJ and normalized to β-actin.

Statistical Analysis

Data are presented as means ± standard deviation and analyzed using GraphPad Prism 10.1.2. Statistical significance was set at $P < 0.05$. Data were screened for outliers using Grubbs' test. Statistical comparisons between two groups were performed using unpaired, two-tailed Student's t-tests. Multiple group comparisons were conducted using one-way ANOVA followed by Tukey's post hoc tests where indicated.

Results

Ginsenoside Rg1 Ameliorates Cardiopulmonary Hemodynamics in PH Rats

To investigate the effects of Ginsenoside Rg1 on PH, rats were treated with either Ginsenoside Rg1 or Sildenafil (positive control) via oral gavage (Figure 1A and B). Right ventricular systolic pressure (RVSP) was significantly elevated in rats treated with combined hypoxia and Sugen compared to control animals, validating successful establishment of the PH rodent model. Ginsenoside Rg1 treatment dose-dependently reduced RVSP compared to the SuHx group (Figure 1C and D). Echocardiography demonstrated that both tricuspid annular plane systolic excursion (TAPSE) and pulmonary artery acceleration time to ejection time ratio (PAT/PET) were significantly decreased in SuHx rats compared to controls. Ginsenoside Rg1 administration significantly attenuated the hypoxia-induced reductions in TAPSE (Figure 1E and F) and PAT/PET compared to the SuHx model group (Figure 1G and H). These findings highlight the protective role of Ginsenoside Rg1 against PH.

Ginsenoside Rg1 Improves Pulmonary Vascular Remodeling in Sugen/Hypoxia-Induced PH Rat

Pulmonary vascular remodeling was assessed by measuring the percentage of vessel wall thickness (WT%) using HE staining. Compared to the control group, sugen/hypoxia-exposed rats exhibited a significant increase in WT% and medial layer thickening of the pulmonary arteries. However, treatment with Ginsenoside Rg1 significantly attenuated these vascular changes (Figure 2A and B). Proliferation of PASMCs within the medial layer was evaluated using dual immunofluorescence staining for α-SMA (red) and PCNA (green). The SuHx group demonstrated significantly enhanced co-localization of α-SMA and PCNA in pulmonary arterial sections compared to controls, indicating increased PASMC proliferation. Furthermore, Ginsenoside Rg1 administration resulted in a reduction in α-SMA and PCNA co-localization (Figure 2C and D). These findings indicate that Ginsenoside Rg1 effectively inhibits PASMC proliferation, thereby attenuating PVR.

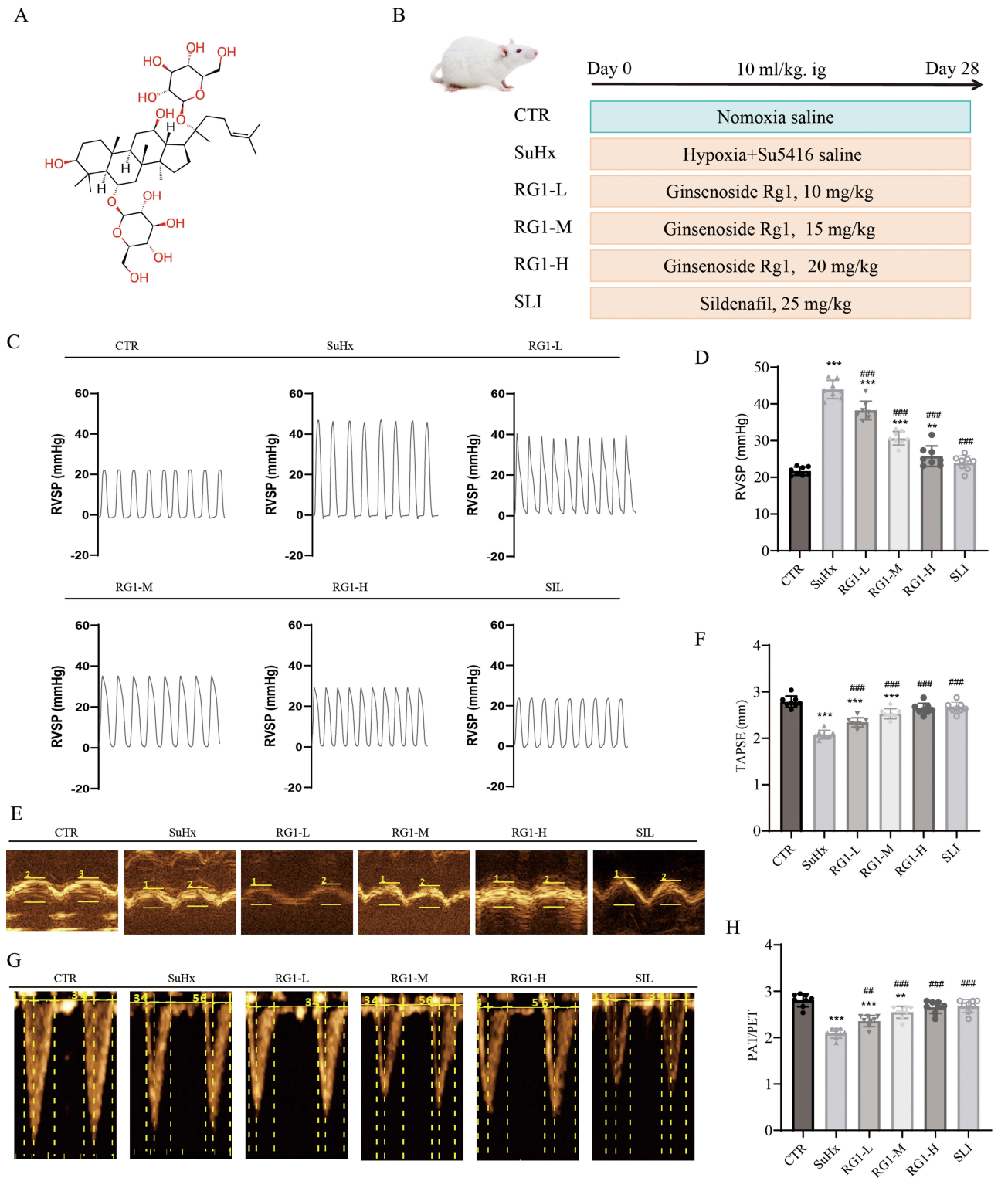

Figure 1 Ginsenoside Rg1 attenuates hemodynamics in Su/Hx rats. (**A** and **B**) Sildenafil (25 mg/kg) or different doses of ginsenoside Rg1 (10, 15, 20 mg/kg) were given by gavage to Sugen/hypoxia-treated rats. (**C**) Measurement of right ventricular systolic pressure (RVSP) by right heart catheterization in different groups. (**D**) Quantification of RVSP, indicating the effect of RG1 treatment. (**E**) Representative echocardiographic images showing tricuspid annular plane systolic excursion (TAPSE). (**F**) Bar graphs depicting TAPSE measurements. (**G**) Echocardiogram demonstrating pulmonary artery acceleration time (PAT) and pulmonary ejection time (PET). (**H**) Quantitative data represent PAT/PET analysis. The results are presented as the mean ± SD, n=8. One-way ANOVA with Tukey's post-hoc test. $^{**}P < 0.01$ and $^{***}P < 0.001$ *versus* control group; $^{\#\#}P < 0.01$, $^{\#\#\#}P < 0.001$, *versus* Su/Hx group.

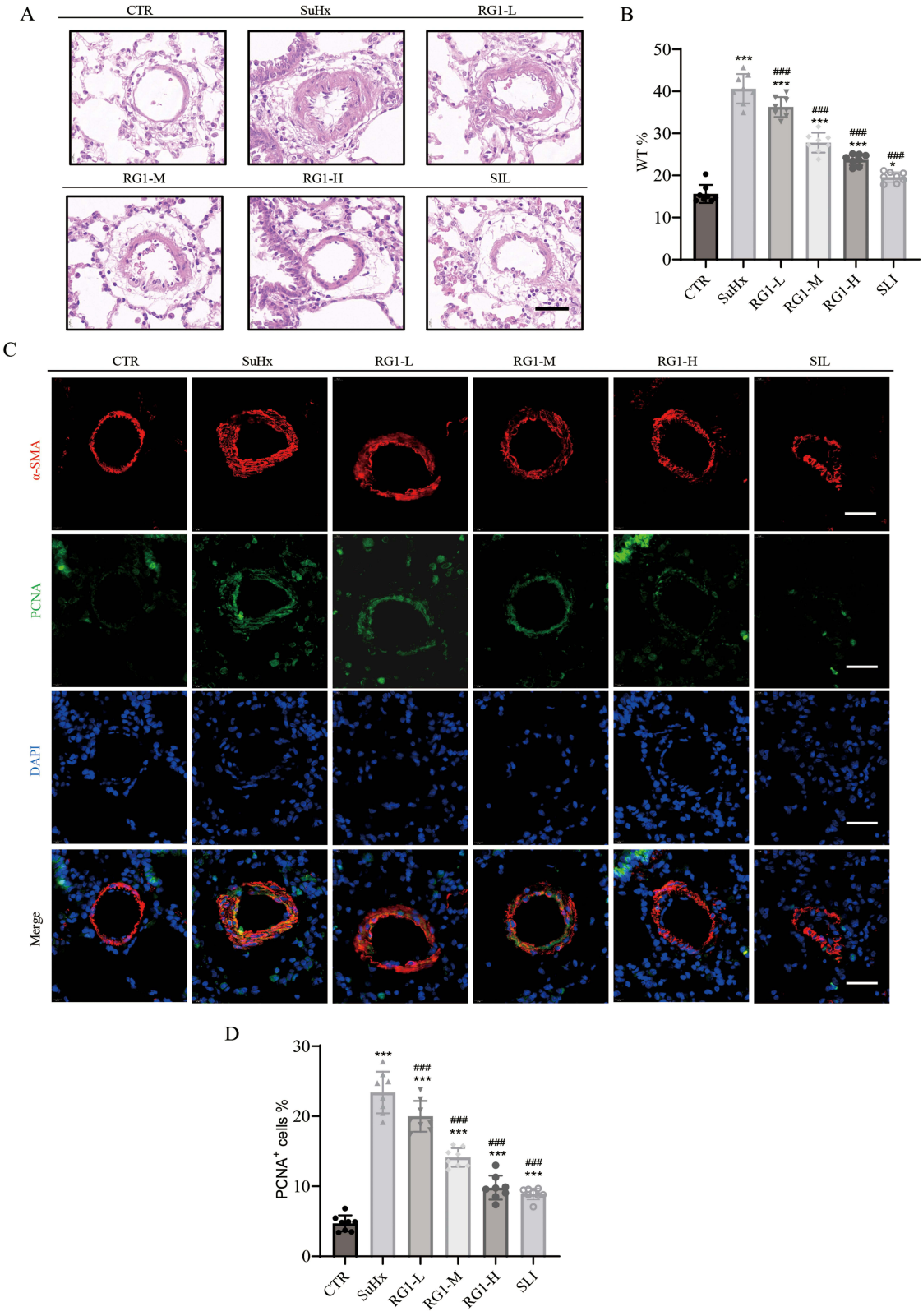

Figure 2 Ginsenoside Rg1 reverses pulmonary vascular remodeling in pulmonary hypertension. (**A**) HE-stained lung sections assessing the thickness of the middle layer of the pulmonary artery, Scale bar = 50μm. (**B**) Statistical chart of pulmonary artery wall thickness. (**C**) Immunofluorescence co-localization of α-SMA and PCNA reveals pathological changes in pulmonary artery smooth muscle cells, Scale bar = 40μm. (**D**) Quantitative Analysis of PCNA-positive vascular cells. The results are presented as the mean ± SD, n=8. One-way ANOVA with Tukey's post-hoc test. $^{*}P < 0.05$ and $^{***}P < 0.001$ *versus* control group, $^{\#\#\#}P < 0.001$, *versus* Su/Hx group.

https://doi.org/10.2147/DDDT.S527938

Ginsenoside Rg1 Attenuates Right Ventricular Hypertrophy in PH Rat Model

To evaluate the effects of ginsenoside Rg1 on right ventricular remodeling during PH progression, small animal echocardiography was utilized to assess structural and functional alterations in the right ventricle of experimental rats. RVAWT was significantly elevated in the SuHx group compared to controls, indicating right ventricular hypertrophy (Figure 3A and B). This pathological change was diminished by ginsenoside Rg1 administration. Fulton's index also revealed more severe right ventricular hypertrophy in hypoxia-exposed rats compared to normoxic controls. However, ginsenoside Rg1 treatment attenuated hypoxia-induced right ventricular hypertrophy (Figure 3C). WGA staining demonstrated increased right ventricular cardiomyocyte volume in hypoxic rats, which was reversed by ginsenoside Rg1 administration (Figure 3D and E). Collectively, these findings indicate that ginsenoside Rg1 effectively prevents right ventricular remodeling induced by combined hypoxia and SU5416 treatment.

Identification of Potential Targets of Ginsenoside Rg1 Against PH and Functional Enrichment Analysis

The GeneCards and OMIM platforms identified 9525 differentially expressed genes associated with PH. A total of 104 potential therapeutic targets of ginsenoside Rg1 were predicted through SwissTarget Prediction, SEA database searches, and literature review. Intersection analysis of disease- and drug-related targets revealed 92 overlapping targets (Figure 4A). The STRING database was employed to construct a PPI network, which was imported into Cytoscape to generate a PPI network comprising 92 nodes and 730 edges. The top 30 targets with the degree value of IL6, AKT1, EGFR, SRC, STAT3, STING, NFKB1, PPARG, MMP9, IL2, and cGAS were selected as the hub targets of ginsenoside Rg1 against PH (Figure 4B). Subsequently, functional enrichment and gene annotation analyses were conducted using the DAVID database. The KEGG pathway enrichment analysis revealed significant enrichment in the HIF-1 signaling pathway, FoxO signaling pathway, and cellular senescence pathways (Figure 4C and D). Molecular docking analyses demonstrated significant binding interaction between ginsenoside Rg1 and cGAS (Figure 4E). Therefore, we identified the cGAS-STING signaling pathway, SASP, and cellular senescence processes as pivotal mechanisms underlying the therapeutic effects of ginsenoside Rg1 in PH based on the network pharmacology findings.

Ginsenoside Rg1 Suppresses the cGAS/STING Signaling Pathway in vivo

To investigate the molecular mechanisms mediating the protective effects of ginsenoside Rg1 against pulmonary hypertension, we analyzed key signaling proteins in lung tissues from control and Sugen/hypoxia-treated animals. Given the integrated findings from network pharmacology and bioinformatics analyses, we proceeded to validate the expression of cGAS and STING in rodent PH models. Pulmonary cGAS and STING mRNA expression was significantly elevated in Sugen/hypoxia-treated rats, whereas ginsenoside Rg1 markedly reversed these elevations (Figure 5A and B). Subsequent Western blot analysis confirmed these findings at the protein level. In the pulmonary tissue of SuHx rats, the expression levels of cGAS, STING, p-STING, TBK1, and p-TBK1 were significantly upregulated compared to those in control groups. The administration of ginsenoside Rg1 notably reduced the protein levels Figure 5C–H). Immunofluorescence analysis revealed significantly elevated cGAS and STING expression in pulmonary arteries of SuHx rats compared to controls, which was markedly attenuated by ginsenoside Rg1 administration (Figure 5I–L). These findings reveal that ginsenoside Rg1 represses cGAS-STING pathway activation in pulmonary tissues of rats with PH.

Ginsenoside Rg1 Alleviates Cellular Senescence and SASP Expression in PH

To investigate the regulatory effects of ginsenoside Rg1 on cellular senescence, we analyzed the senescence markers p16 and p21 using RT-PCR, Western blot and immunohistochemistry. The mRNA levels of both p16 and p21 were significantly elevated in Sugen/hypoxia-treated animals compared to controls, while ginsenoside Rg1 administration attenuated these elevations (Figure 6A and B). Protein expression patterns paralleled the observed mRNA changes. Western blotting demonstrated a significant upregulation of p16 and p21 in SuHx-treated animals, which was reduced by ginsenoside Rg1 (Figure 6C–E). Additionally, immunohistochemical analysis yielded consistent staining patterns (Figure 6F–I). These findings demonstrate that ginsenoside Rg1 mitigates pulmonary hypertension-associated cellular

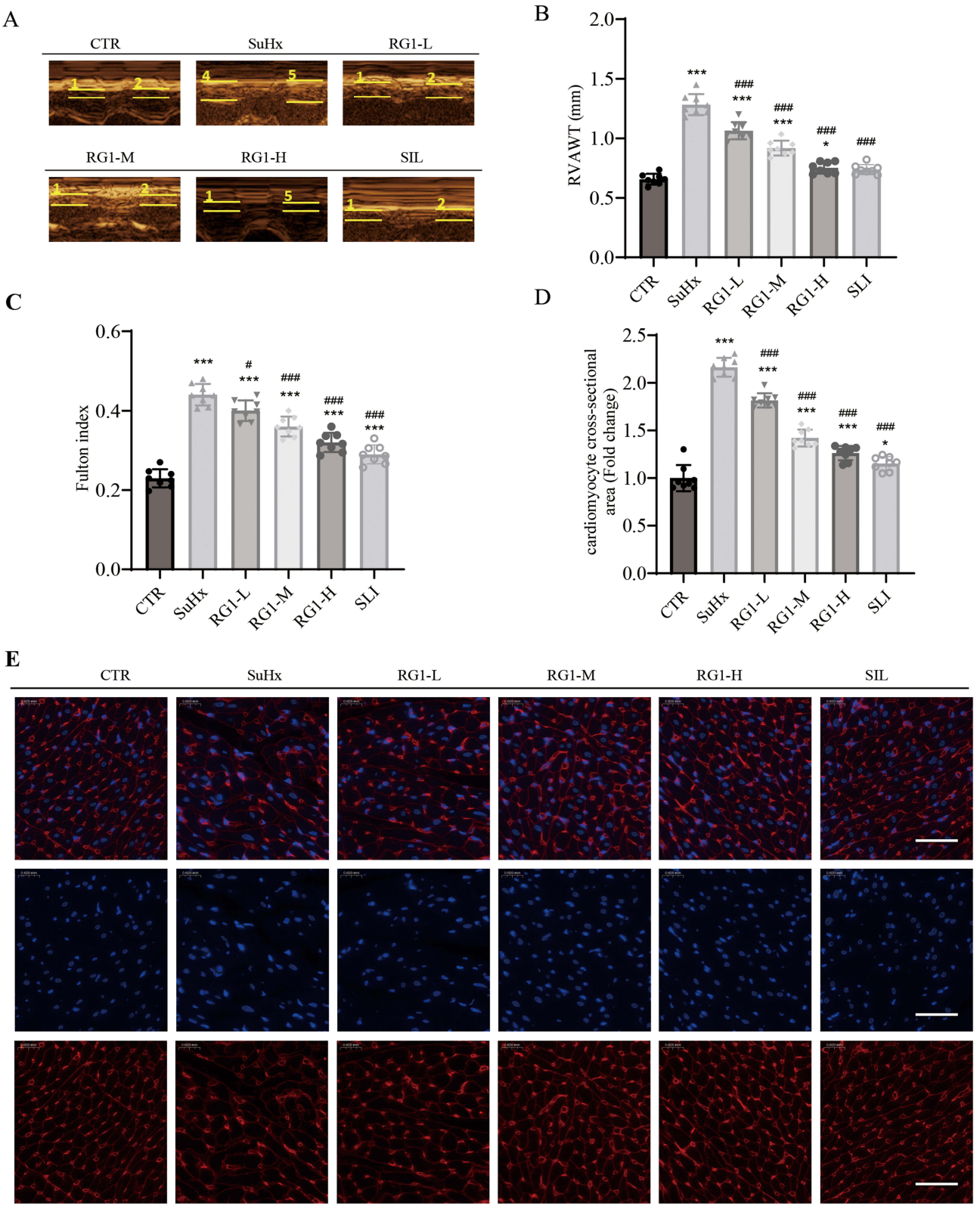

Figure 3 Ginsenoside Rg1 improves right ventricular function and structure in *vivo*. (**A**) Typical graphic and of right ventricle anterior wall thickness (RVAWT) by echocardiography, Scale bar = 40μm. (**B**) Statistical analysis of RVAWT. (**C**) Fulton index assessing the effect of rg1 in right ventricular hypertrophy. (**D**–**E**) WGA staining evaluating right ventricular cardiomyocyte volume changes and quantitative cardiomyocyte cross-sectional area ratio, Scale bar = 40μm. The results are presented as the mean ± SD, n=8. One-way ANOVA with Tukey's post-hoc test. $^{*}P < 0.05$ and $^{***}P < 0.001$ *versus* control group, $^{\#}P < 0.05$ and $^{\#\#\#}P < 0.001$, *versus* Su/Hx group.

https://doi.org/10.2147/DDDT.S527938

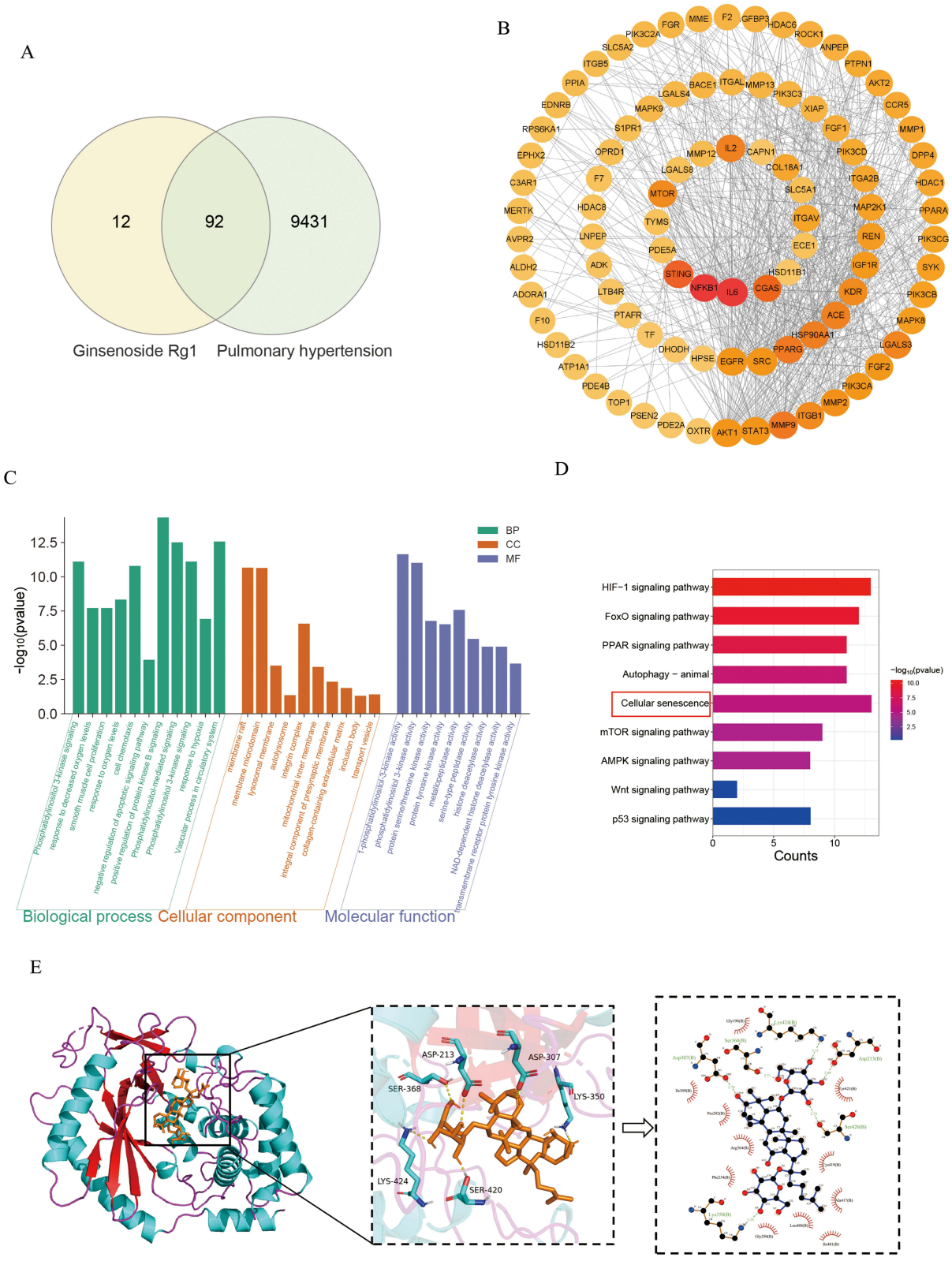

Figure 4 Network pharmacology was employed to investigate the therapeutic mechanisms of Ginsenoside Rg1 in treating pulmonary hypertension. (**A**) Venn diagram to identify overlapping therapeutic targets between ginsenoside Rg1 and pulmonary hypertension. (**B**) PPI network analysis of intersection targets was conducted to identify core therapeutic regulators. (**C**) GO enrichment analysis. (**D**) KEGG pathway enrichment analysis. (**E**) Docking analysis of ginsenoside Rg1 with cGAS.

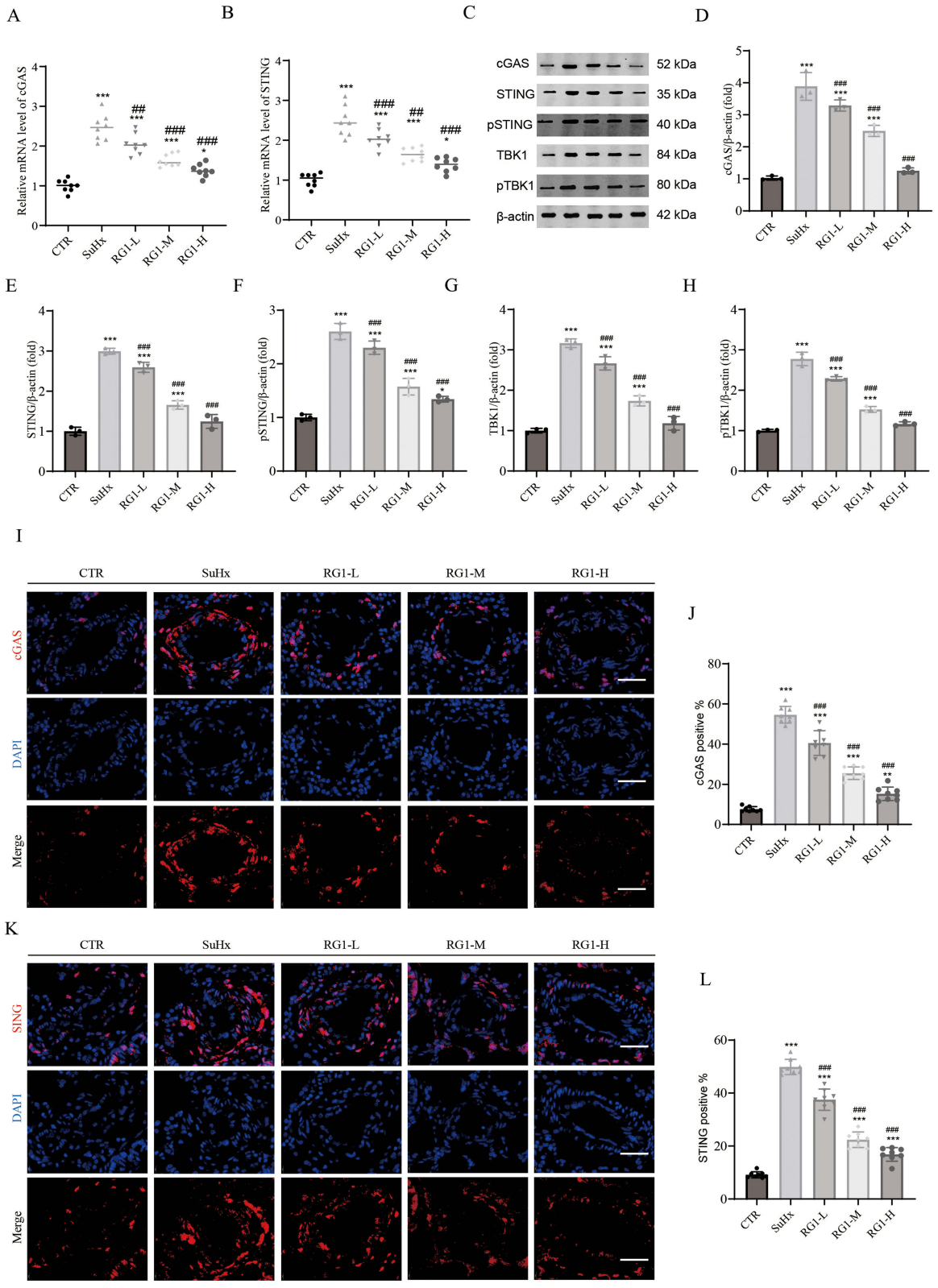

Figure 5 Ginsenoside Rg1 represses activation of the cGAS/STING pathway in Su/Hx models. (**A** and **B**) The relative mRNA expression of cGAS and STING, n=8. (**C**) Representative Western blots of cGAS, STING, pSTING, TBK1, and pTBK1. (**D**–**H**) Quantification of protein expression levels of cGAS, STING, pSTING, TBK1, and pTBK1, n=3. (**I**) Representative immunofluorescence images of cGAS in pulmonary arteries, Scale bar = 40μm. (**J**) Quantitative analysis of cGAS-positive vascular cells, n=8. (**K**) Representative immunofluorescence images of STING in pulmonary arteries, Scale bar = 40μm. (**L**) Quantitative analysis of STING-positive vascular cells, n=8. The results are presented as the mean ± SD. One-way ANOVA with Tukey's post-hoc test. **P* < 0.05, ***P* < 0.01 and ****P* < 0.001 *versus* control group, $^{\#\#}P$ < 0.01 and $^{\#\#\#}P$ < 0.001, *versus* Su/Hx group.

https://doi.org/10.2147/DDDT.S527938

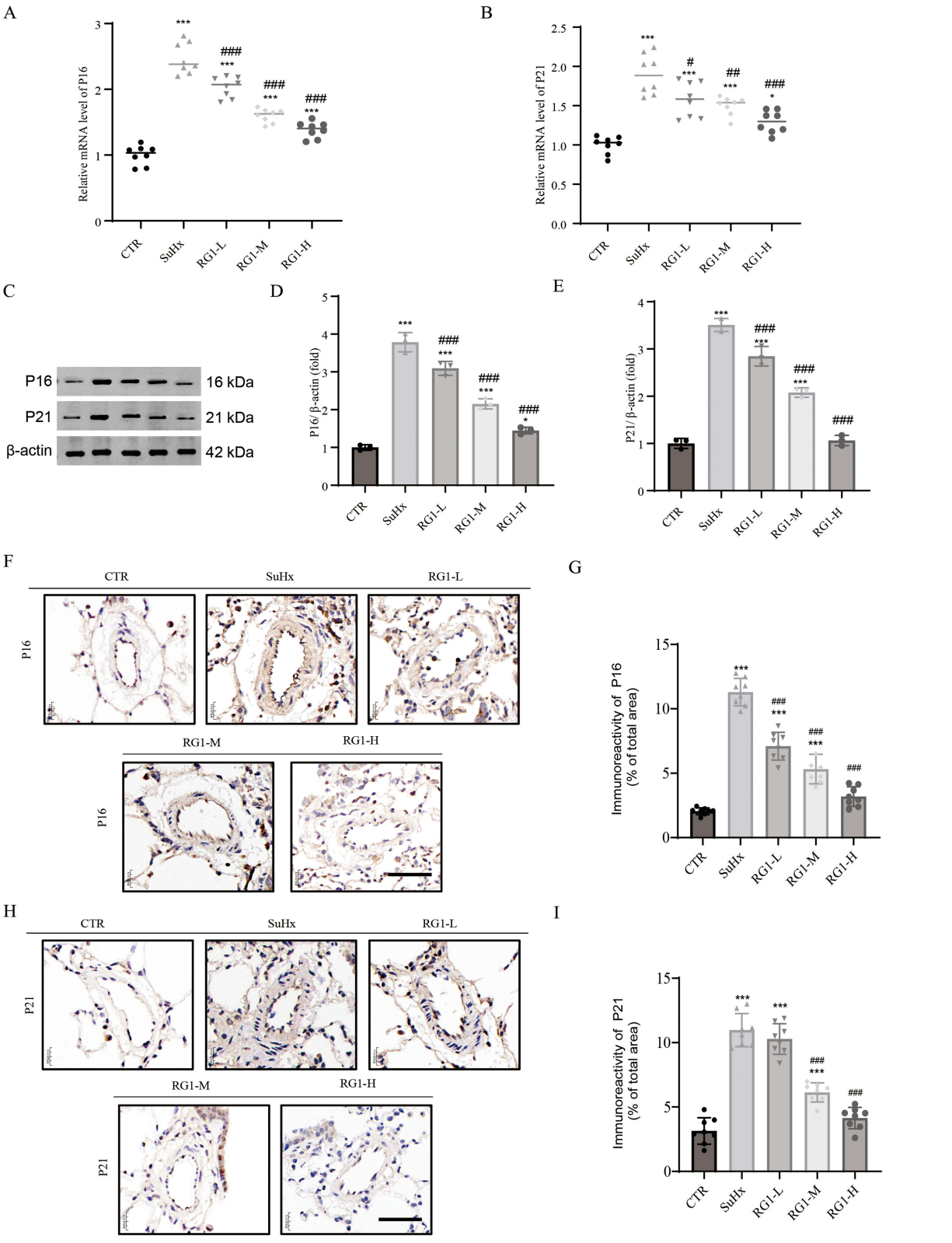

Figure 6 Ginsenoside Rg1 modulates cellular senescence in pulmonary arterial cells from hypoxia/su5416-induced rats. (**A** and **B**) The relative mRNA expression of p16 and p21. (**C**) Representative Western blots of p16 and p21. (**D** and **E**) Quantification of protein expression levels of p16 and p21, n=3. (**F**) Representative immunohistochemical staining of p16 expression in lung sections, Scale bar = 40μm. (**G**) Statistical analysis of p16-positive vascular cells, n=8. (**H**) Representative immunohistochemical staining of p21 expression in lung sections, Scale bar = 40μm. (**I**) Statistical analysis of p21-positive vascular cells, n=8. The results are presented as the mean ± SD. One-way ANOVA with Tukey's post-hoc test. **P* < 0.05 and ****P* < 0.001 *versus* control group, $^{\#}P$ < 0.05, $^{\#\#\#}P$ < 0.01, $^{\#\#\#\#}P$ < 0.001, *versus* Su/Hx group.

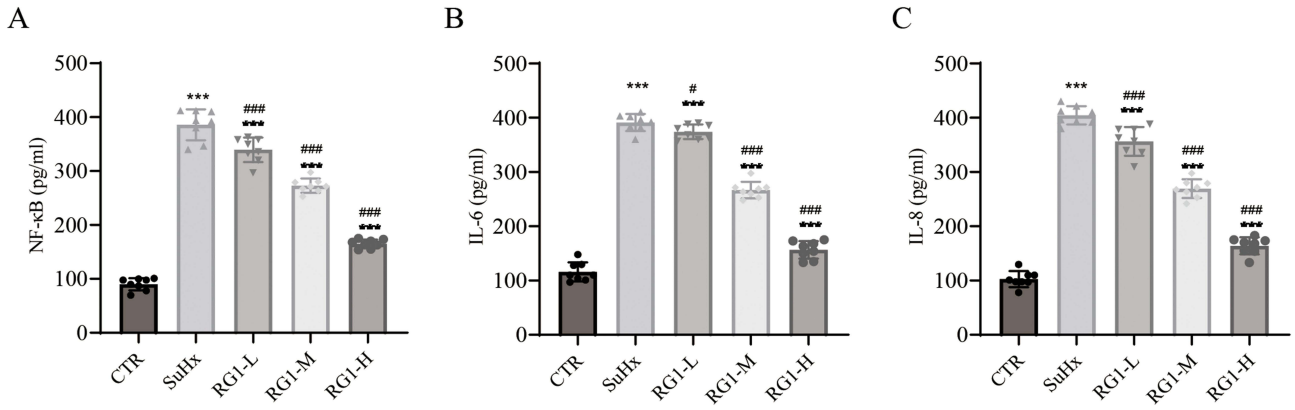

Figure 7 Ginsenoside Rg1 inhibits senescence-associated secretory phenotype in PH rat. (**A**) Plasma NF-kB levels under various experimental conditions in rats. (**B**) Plasma IL6 levels under various experimental conditions in rats. (**C**) Plasma IL8levels under various experimental conditions in rats. The results are presented as the mean ± SD, n=8. One-way ANOVA with Tukey's post-hoc test. ***$P < 0.001$ *versus* control group, #$P < 0.05$ and ###$P < 0.001$, *versus* Su/Hx group.

senescence through modulation of senescence marker expression. To evaluate the effects of ginsenoside Rg1 on the SASP, we quantified plasma levels of NF-κB, IL-6, and IL-8 using ELISA (Figure 7A–C). Ginsenoside Rg1 significantly suppressed the secretion of these inflammatory mediators. These findings support that ginsenoside Rg1 attenuates cellular senescence in rats with Sugen/hypoxia-induced pulmonary hypertension through SASP inhibition.

Ginsenoside Rg1 Exhibits a Favorable Safety Profile in PH Rats

To evaluate the biosafety profile of Rg1 administration, hematological analysis and hepatic/renal function assessments were performed. Quantitative analysis revealed no statistically significant alterations in body weight and complete blood count parameters between the Rg1-treated and control groups (P>0.05, Figure 8A and B. Similarly, critical indexes including ALT, AST, BUN, and Cr were not significantly different across several groups (P>0.05, Figure 8C and D). Histopathological examination via HE staining further corroborated these findings, showing tissue architecture in liver, spleen, and kidney with no evidence of pathological alterations (Figure 8E–G).

Discussion

PH is a globally recognized disease that poses a significant threat to human health, with its complex pathogenesis presenting substantial challenges for clinical diagnosis and treatment. The pathophysiological mechanisms of PH involve multiple factors, including vascular endothelial cell injury, abnormal smooth muscle cell proliferation, inflammatory responses, and thrombosis. These interconnected pathophysiological processes induce both structural and functional alterations in the pulmonary vasculature, consequently leading to elevated pulmonary vascular resistance and right ventricular dysfunction. Although the exact pathogenesis of PH remains unclear, current evidence suggests that its development involves multiple molecular pathways, including genetic mutations, epigenetic modifications, and environmental factors. Pathogenic factors associated with PH can trigger accelerated cellular senescence, and epidemiological studies demonstrate significantly elevated incidence and mortality rates among elderly populations. These observations strongly indicate that cellular senescence serves as a crucial mediator in PH pathogenesis. Current therapeutic options for PH, including endothelin receptor antagonists, phosphodiesterase-5 inhibitors, prostacyclin analogs, and soluble guanylate cyclase agonists, primarily function by regulating pulmonary vascular tone and modulating vascular cell proliferation. These agents provided some improvement in clinical symptoms, with no reduction in disease progression or mortality. Therefore, there is an urgent need to develop new therapeutic strategies, and cellular senescence may be an important direction to effectively target vascular remodeling in PH.

Ginsenoside Rg1, a principal bioactive constituent of ginseng, has garnered significant scientific interest for its potent anti-senescent effects.[35,36] Ginsenoside Rg1 exhibits robust antioxidant properties in age-related disorders by reducing ROS levels, downregulating NOX2 expression, and enhancing SOD activity, thereby mitigating ROS production and

https://doi.org/10.2147/DDDT.S527938

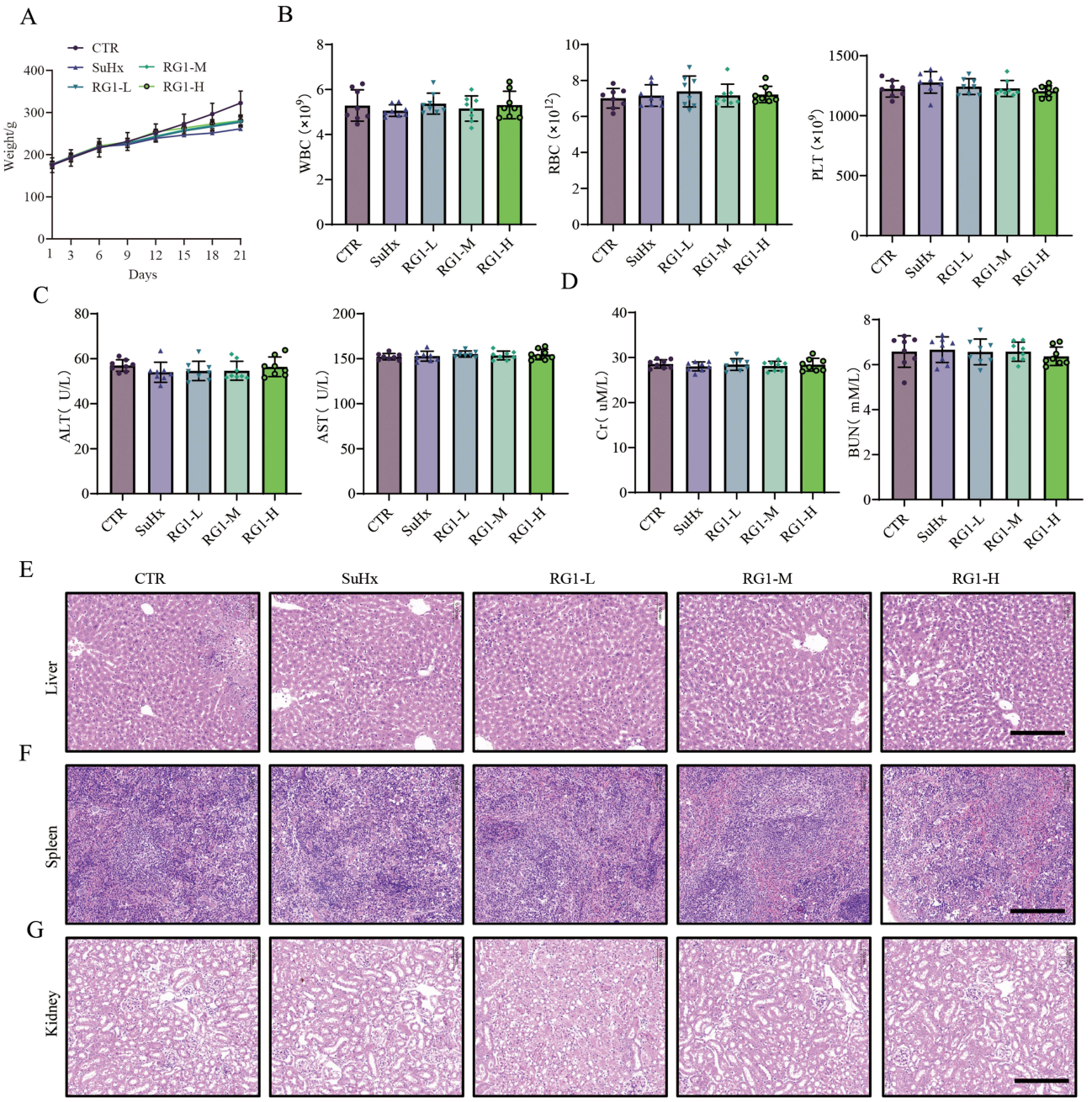

Figure 8 Biosafety assessment of Ginsenoside Rg1 in *vivo*. (**A**) Body weight in rats. (**B**) Quantitative hematological profiling, including leukocyte count, erythrocyte count, and platelet count. (**C** and **D**) Hepatic transaminases ALT/AST and renal functional markers Cr/ BUN. (**E**–**G**) Histopathological evaluation by HE staining of hepatic, splenic, and renal tissues. The results are presented as the mean ± SD, n=8. One-way ANOVA with Tukey's post-hoc test.

mitochondrial damage.[37–39] In coronary artery disease, Rg1 improves endothelial cell viability and attenuates cellular senescence and oxidative stress via the AMPK/SIRT3/p53 signaling cascade.[40] Furthermore, Rg1 promotes cell proliferation and differentiation while facilitating senescent cell repair and renewal by enhancing regenerative capacity.[41,42] It also suppresses hypoxia-induced inflammation, fibrosis, and cell proliferation through inhibition of the calpain-1/STAT3 signaling pathway, effectively attenuating vascular remodeling.[43] Additionally, Rg1 ameliorates hypoxia-induced PH by upregulating CCN1, which suppresses proinflammatory cytokines TNF-α and IL-1β and inhibits endothelial-to-mesenchymal transition.[32] Although recent studies highlight Rg1's therapeutic potential for PH, its anti-PH effects mediated by cellular senescence modulation remain to be elucidated.

In the present study, a SuHx-induced PH rat model was established and characterized using right heart catheterization, echocardiography, and pathological examination. The SuHx rat model was found to show typical characteristic features of PH, such as increased RVSP and decreased PAT/PET and TAPSE, identifying cardiopulmonary hemodynamic abnormalities; increased right heart cardiomyocyte volume confirming the pathological changes of right heart hypertrophy; and a significant increase in the relative thickness of the intima-media smooth muscle layer of the small pulmonary blood vessels, which is consistent with the pathomorphological changes of the small arterioles in the lung tissues of PH. The current study proved the therapeutic efficacy of ginsenoside Rg1 in PH by using different concentrations of ginsenoside Rg1 in vivo, as evidenced by improved pulmonary hemodynamics, enhanced right ventricular function, and reduced vascular remodeling. To elucidate the underlying mechanisms, we demonstrated that the cGAS/STING pathway is associated with PVR in PH by using RT-PCR and immunofluorescence, and that ginsenoside Rg1 exerts its protective effects by inhibiting this signaling pathway. Ginsenoside Rg1 treatment significantly suppressed the hypoxia-induced expression of senescence-associated proteins p16 and p21. These findings demonstrate that ginsenoside attenuates PVR through dose-dependent inhibition of cellular senescence, suggesting its therapeutic potential for PH.

The cGAS-STING pathway serves as a significant trigger for cellular senescence.[44,45] In MCT-induced rodent PH models, mRNA and protein levels of cGAS and STING were significantly upregulated in lung tissues.[22,23] STING exacerbates vascular remodeling by promoting the activation of NLRP3 inflammasome in macrophages, driving inflammatory response and cell proliferation in PH.[46] TBK1 is the key kinase recruited by activated STING and drive downstream interferon and SASP responses.[47] pTBK1 mediates cGAS/STING activation and chondrocyte senescence, while BX795 inhibits TBK1 to disrupt this pathway and attenuate inflammation and senescence in osteoarthritis.[48] In senescent cells, cytoplasmic chromatin fragments are recognized by cGAS, triggering the cGAS-STING pathway and inducing robust SASP factor production, which promotes paracrine senescence.[49] Senescent cells secrete interleukin-6 (IL-6), a key SASP factor, interacting with its receptor to activate the cytoplasmic DNA signaling pathway, subsequently triggering the cGAS-STING pathway and NF-κB.[50] This cascade not only amplifies senescence in SASP-producing cells but also spreads senescence signals to neighboring cells via paracrine effects, promoting their proliferation. Consequently, this process propagates senescence signals throughout the cell population, exacerbating cellular senescence. Our data demonstrated that ginsenoside Rg1 significantly reduced plasma concentrations of SASP markers (NF-κB, IL-6, and IL-8) in SuHx-induced PH rats. These findings offer new insights into the molecular mechanisms underlying the beneficial effects of ginsenoside Rg1, while simultaneously elucidating the crucial role of the cGAS/STING signaling pathway in the process of cellular senescence.

To further corroborate ginsenoside Rg1's anti-PH mechanism, we will next conduct in *vitro* studies using primary PASMCs subjected to hypoxic condition. We will manipulate cGAS/STING activity via siRNA knockdown and selective pharmacological agonists/antagonists to directly validate ginsenoside Rg1's effects on senescence-associated markers and downstream signaling pathways. Concurrently, dose–response optimization experiments will be performed to define a sustainable long-term dosing regimen, and translational potential will be evaluated in multiple animal species through comprehensive pharmacokinetic profiling and biomarker development. This integrated approach will accelerate the advancement of ginsenoside Rg1 from mechanistic investigation toward a novel therapeutic candidate for PH.

Conclusion

In conclusion, this study demonstrates that ginsenoside Rg1 reverses vascular remodeling in a PH model induced by Sugen treatment combined with hypoxia. Ginsenoside Rg1 suppressed the activation of the cGAS-STING pathway in Su/Hx rats, thereby inhibiting the secretion of SASP molecules and cellular senescence. These findings elucidate the mechanism through which ginsenoside Rg1 ameliorates vascular remodeling by inhibiting the cGAS-STING pathway and cellular senescence, providing new insights into the potential of ginsenoside Rg1 as a natural therapeutic agent for senescence-related diseases.

Data Sharing Statement

The data supporting the findings of this study are available from the corresponding author upon reasonable request.

Ethics Approval

The study was performed according to the protocol approved by the Ethics Committee of The First Hospital of Hunan University of Chinese Medicine, Changsha, China (Registration number: LLBH-202311020006).

Acknowledgments

We express our gratitude to the staff of the Institutional Key Laboratory of Vascular Biology and Translational Medicine of Hunan University of Chinese Medicine.

Author Contributions

All authors made a significant contribution to the work reported, whether that is in the conception, study design, execution, acquisition of data, analysis and interpretation, or in all these areas; took part in drafting, revising, or critically reviewing the article; gave final approval of the version to be published; have agreed on the journal to which the article has been submitted; and agree to be accountable for all aspects of the work.

Funding

This work was funded by the National Natural Science Foundation of China (82370069), the Youth Fund of Natural Science Foundation of Hunan Province (2024JJ6339), Hunan Provincial Department of Education Outstanding Youth Project (22B0383), Hunan Province Science and Technology Research Project (2023SK2089), Changsha Natural Science Foundation (kq2208184) and National Key Laboratory Cultivation Base of Chinese Medicinal Powder and Innovative Medicinal Jointly Established by Province and Ministry Foundation (2022FTKFJJ01).

Disclosure

The authors declare that they have no conflicts of interest in this work.

References

1. Mocumbi A, Humbert M, Saxena A, et al. Pulmonary hypertension. *Nat Rev Dis Prim*. 2024;10(1):1. doi:10.1038/s41572-023-00486-7
2. Chin KM, Gaine SP, Gerges C, et al. Treatment algorithm for pulmonary arterial hypertension. *Europ Resp J*. 2024;64(4). doi:10.1183/13993003.01325-2024
3. Fukumoto Y. Pathophysiology and treatment of pulmonary arterial hypertension. *Int J Mol Sci*. 2024;25(2). doi:10.3390/ijms25021166
4. Li X, Tan J, Wan J, Cheng B, Wang YH, Dai A. Cell death in pulmonary arterial hypertension. *Int J Med Sci*. 2024;21(10):1840–1851. doi:10.7150/ijms.93902
5. Shlobin OA, Adir Y, Barbera JA, et al. Pulmonary hypertension associated with lung diseases. *Europ Resp J*. 2024;64(4). doi:10.1183/13993003.01200-2024
6. Kovacs G, Bartolome S, Denton CP, et al. Definition, classification and diagnosis of pulmonary hypertension. *Europ Resp J*. 2024;64(4). doi:10.1183/13993003.01324-2024
7. de Magalhães JP. Cellular senescence in normal physiology. *Science*. 2024;384(6702):1300–1301. doi:10.1126/science.adj7050
8. Dierick JF, Eliaers F, Remacle J, et al. Stress-induced premature senescence and replicative senescence are different phenotypes, proteomic evidence. *Biochem Pharmacol*. 2002;64(5–6):1011–1017. doi:10.1016/s0006-2952(02)01171-1
9. Reimann M, Lee S, Schmitt CA. Cellular senescence: neither irreversible nor reversible. *J Exp Med*. 2024;221(4). doi:10.1084/jem.20232136
10. Volonte D, Benson CJ, Daugherty SL, Beckel JM, Trebak M, Galbiati F. Purinergic signaling promotes premature senescence. *J Biol Chem*. 2024;300(4):107145. doi:10.1016/j.jbc.2024.107145
11. Qin T, Chen T, Ma R, et al. Stress hormones: unveiling the role in accelerated cellular senescence. *Aging Dis*. 2024. doi:10.14336/ad.2024.0262
12. Lazzarini E, Lodrini AM, Arici M, et al. Stress-induced premature senescence is associated with a prolonged QT interval and recapitulates features of cardiac aging. *Theranostics*. 2022;12(11):5237–5257. doi:10.7150/thno.70884
13. Liu L, Wei Y, Giunta S, He Q, Xia S. Potential role of cellular senescence in pulmonary arterial hypertension. *Clin Exp Pharmacol Physiol*. 2022;49(10):1042–1049. doi:10.1111/1440-1681.13696
14. Safaie Qamsari E, Stewart DJ. Cellular senescence in the pathogenesis of pulmonary arterial hypertension: the good, the bad and the uncertain. *Front Immunol*. 2024;15:1403669. doi:10.3389/fimmu.2024.1403669
15. Wang B, Han J, Elisseeff JH, Demaria M. The senescence-associated secretory phenotype and its physiological and pathological implications. *Nat Rev Mol Cell Biol*. 2024;25(12):958–978. doi:10.1038/s41580-024-00727-x
16. van der Feen DE, Bossers GPL, Hagdorn QAJ, et al. Cellular senescence impairs the reversibility of pulmonary arterial hypertension. *Sci Trans Med*. 2020;12(554). doi:10.1126/scitranslmed.aaw4974
17. Dvorkin S, Cambier S, Volkman HE, Stetson DB. New frontiers in the cGAS-STING intracellular DNA-sensing pathway. *Immunity*. 2024;57(4):718–730. doi:10.1016/j.immuni.2024.02.019
18. Zhang Q, Shen L, Ruan H, Huang Z. cGAS-STING signaling in cardiovascular diseases. *Front Immunol*. 2024;15:1402817. doi:10.3389/fimmu.2024.1402817

19. Yu L, Liu P. cGAS/STING signalling pathway in senescence and oncogenesis. *Semi Cancer Biol*. 2024;106-107:87–102. doi:10.1016/j.semcancer.2024.08.007
20. Wei M, Li Q, Li S, Wang D, Wang Y. Multifaceted roles of cGAS-STING pathway in the lung cancer: from mechanisms to translation. *PeerJ*. 2024;12:e18559. doi:10.7717/peerj.18559
21. Feng Q, Xu X, Zhang S. cGAS-STING pathway in systemic lupus erythematosus: biological implications and therapeutic opportunities. *Immunol Res*. 2024;72(6):1207–1216. doi:10.1007/s12026-024-09525-1
22. Yan X, Huang J, Zeng Y, et al. CGRP attenuates pulmonary vascular remodeling by inhibiting the cGAS-STING-NFκB pathway in pulmonary arterial hypertension. *Biochem Pharmacol*. 2024;222:116093. doi:10.1016/j.bcp.2024.116093
23. Li J, Meng ZY, Wen H, et al. β-sitosterol alleviates pulmonary arterial hypertension by altering smooth muscle cell phenotype and DNA damage/cGAS/STING signaling. *Phytomedicine*. 2024;135:156030. doi:10.1016/j.phymed.2024.156030
24. Ito H, Ito M. Recent trends in ginseng research. *J Nat Med*. 2024;78(3):455–466. doi:10.1007/s11418-024-01792-4
25. Fan W, Fan L, Wang Z, et al. Rare ginsenosides: a unique perspective of ginseng research. *J Adv Res*. 2024;66:303–328. doi:10.1016/j.jare.2024.01.003
26. Ratan ZA, Youn SH, Kwak YS, et al. Adaptogenic effects of panax ginseng on modulation of immune functions. *J Ginseng Res*. 2021;45(1):32–40. doi:10.1016/j.jgr.2020.09.004
27. Zhou G, Wang CZ, Mohammadi S, Sawadogo WR, Ma Q, Yuan CS. Pharmacological effects of ginseng: multiple constituents and multiple actions on humans. *Am J Chin Med*. 2023;51(5):1085–1104. doi:10.1142/s0192415x23500507
28. Shi M, Ma J, Jin S, Wang T, Sui Y, Chen L. Effects of saponins Rb(1) and re in American ginseng combined intervention on immune system of aging model. *Front Mol Biosci*. 2024;11:1392868. doi:10.3389/fmolb.2024.1392868
29. Lin LQ, Mao FK, Lin J, Guo L, Yuan WR, Wang BY. Ginsenoside Rg1 induces ferroptosis by regulating the focal adhesion kinase/protein kinase B-forkhead box O3A signaling pathway and alleviates sepsis-induced myocardial damage. *J Physiol Pharmacol*. 2024;75(4). doi:10.26402/jpp.2024.4.04
30. Wu Z, Huang J, Bai X, et al. Ginsenoside-Rg1 mitigates cardiac arrest-induced cognitive damage by modulating neuroinflammation and hippocampal plasticity. *Eur J Pharmacol*. 2023;938:175431. doi:10.1016/j.ejphar.2022.175431
31. Huang C, Xue X, Gong N, Jiang J. Ginsenoside Rg1 suppresses paraquat-induced epithelial cell senescence by enhancing autophagy in an ATG12-dependent manner. *Environ Toxicol*. 2022;37(9):2302–2313. doi:10.1002/tox.23597
32. Tang BL, Liu Y, Zhang JL, Lu ML, Wang HX. Ginsenoside Rg1 ameliorates hypoxia-induced pulmonary arterial hypertension by inhibiting endothelial-to-mesenchymal transition and inflammation by regulating CCN1. *Biomed Pharmacothe*. 2023;164:114920. doi:10.1016/j.biopha.2023.114920
33. National Research Council Committee for the Update of the Guide for the C, Use of Laboratory A. The National Academies Collection: reports funded by National Institutes of Health. In: *Guide for the Care and Use of Laboratory Animals*. National Academies Press (US) Copyright © 2011, National Academy of Sciences; 2011.
34. Ding R, Wang Y, Xu L, et al. QiDongNing induces lung cancer cell apoptosis via triggering P53/DRP1-mediated mitochondrial fission. *J Cell Mol Med*. 2024;28(9):e18353. doi:10.1111/jcmm.18353
35. Shang D, Li Z, Tan X, Liu H, Tu Z. Inhibitory effects and molecular mechanisms of ginsenoside Rg1 on the senescence of hematopoietic stem cells. *Fundament Clinic Pharmacol*. 2023;37(3):509–517. doi:10.1111/fcp.12863
36. Cheng Y, Shen LH, Zhang JT. Anti-amnestic and anti-aging effects of ginsenoside Rg1 and Rb1 and its mechanism of action. *Acta Pharmacol Sin*. 2005;26(2):143–149. doi:10.1111/j.1745-7254.2005.00034.x
37. Han Y, Li X, Yang L, et al. Ginsenoside Rg1 attenuates cerebral ischemia-reperfusion injury due to inhibition of NOX2-mediated calcium homeostasis dysregulation in mice. *J Ginseng Res*. 2022;46(4):515–525. doi:10.1016/j.jgr.2021.08.001
38. Zhang G, Zhang M, Yu J, Kang L, Guan H. Ginsenoside Rg1 prevents H(2)O(2)-induced lens opacity. *Curr Eye Res*. 2021;46(8):1159–1165. doi:10.1080/02713683.2020.1869266
39. Lu M, Zhao F, Ran C, Xu Y, Zhang J, Wang H. Ginsenoside Rg1 attenuates diabetic vascular endothelial dysfunction by inhibiting the calpain-1/ROS/PKC-β axis. *Life Sci*. 2023;329:121972. doi:10.1016/j.lfs.2023.121972
40. Lyu TJ, Zhang ZX, Chen J, Liu ZJ. Ginsenoside Rg1 ameliorates apoptosis, senescence and oxidative stress in ox-LDL-induced vascular endothelial cells via the AMPK/SIRT3/p53 signaling pathway. *Exp Ther Med*. 2022;24(3):545. doi:10.3892/etm.2022.11482
41. He F, Yu C, Liu T, Jia H. Ginsenoside Rg1 as an effective regulator of mesenchymal stem cells. *Front Pharmacol*. 2019;10:1565. doi:10.3389/fphar.2019.01565
42. Xiang Y, Wang SH, Wang L, et al. Effects of ginsenoside Rg1 regulating Wnt/β-catenin signaling on neural stem cells to delay brain senescence. *Stem Cells International*. 2019;2019:5010184. doi:10.1155/2019/5010184
43. Ran C, Lu M, Zhao F, et al. Ginsenoside Rg1 alleviates vascular remodeling in hypoxia-induced pulmonary hypertension mice through the calpain-1/STAT3 signaling pathway. *J Ginseng Res*. 2024;48(4):405–416. doi:10.1016/j.jgr.2024.03.001
44. Loo TM, Miyata K, Tanaka Y, Takahashi A. Cellular senescence and senescence-associated secretory phenotype via the cGAS-STING signaling pathway in cancer. *Cancer Sci*. 2020;111(2):304–311. doi:10.1111/cas.14266
45. Wu Q, Leng X, Zhang Q, et al. IRF3 activates RB to authorize cGAS-STING-induced senescence and mitigate liver fibrosis. *Sci Adv*. 2024;10(9):eadj2102. doi:10.1126/sciadv.adj2102
46. Wu DD, Deng Y, Liao J, Xie SS, Meng H, Lan WF. STING mediates SU5416/hypoxia-induced pulmonary arterial hypertension in rats by regulating macrophage NLRP3 inflammasome activation. *Immunobiology*. 2023;228(2):152345. doi:10.1016/j.imbio.2023.152345
47. Zhang D, Liu Y, Zhu Y, et al. A non-canonical cGAS-STING-PERK pathway facilitates the translational program critical for senescence and organ fibrosis. *Nat Cell Biol*. 2022;24(5):766–782. doi:10.1038/s41556-022-00894-z
48. Lu R, Qu Y, Wang Z, et al. TBK1 pharmacological inhibition mitigates osteoarthritis through attenuating inflammation and cellular senescence in chondrocytes. *J Orthopaedic Translation*. 2024;47:207–222. doi:10.1016/j.jot.2024.06.001
49. Glück S, Guey B, Gulen MF, et al. Innate immune sensing of cytosolic chromatin fragments through cGAS promotes senescence. *Nat Cell Biol*. 2017;19(9):1061–1070. doi:10.1038/ncb3586
50. Herbstein F, Sapochnik M, Attorresi A, et al. The SASP factor IL-6 sustains cell-autonomous senescent cells via a cGAS-STING-NFκB intracrine senescent noncanonical pathway. *Aging Cell*. 2024;23(10):e14258. doi:10.1111/acel.14258